Optik - International Journal for Light and Electron Optics 203 (2020) 164017

Contents lists available at ScienceDirect

Optik

journal homepage: www.elsevier.com/locate/ijleo

Original research article

Thermal design and test verification of the solar X-Ray and extreme ultraviolet imager

Shijun Li[a,b], Liheng Chen[a,*,1], Yuting Yang[a,b,2]

[a] Changchun Institute of Optics, Fine Mechanics and Physics, Chinese Academy of Sciences, Changchun, Jilin, 130033, China
[b] University of Chinese Academy of Sciences, Beijing, 100049, China

ARTICLE INFO

Keywords:
Thermal design
Thermal control
CCD
Thermal balance test

ABSTRACT

This paper describes a detailed thermal design scheme to ensure the low-temperature detection requirements of the solar X-ray and extreme ultraviolet imager (XEUVI) under complex external heat flux conditions. First, the structure, working mode and internal heat sources of the imager are introduced. Second, the thermal design scheme is proposed with a combination of active and passive thermal controls. Finally, a thermal balance test of XEUVI was performed in a vacuum environment. The test results showed that the CCD temperature ranged from -65.6°C to -56.3°C, the optical system temperature ranged from 12.9°C to 22.0°C, the frame temperature ranged from -4.6°C to 20.3°C, the motor temperature ranged from 1.0°C to 19.8°C, and the electrical box temperature ranged from -2°C to 38.8°C. The results of testing meet the requirements of the thermal control indices, and the thermal balance test verifies the correctness of the thermal design.

1. Introduction

The sun is the disturbance source of space weather. Coronal mass ejection, flares, coronal holes, and other activity during a solar burst are the sources of magnetic storms, ionospheric disturbance, and high-speed solar wind, which have a great impact on all aspects of human space activities [1]. Therefore, the observation of solar activity phenomena has become a broad-based and urgent need.

Solar activity phenomena in the corona and the chromosphere are intense, and solar radiation is mainly concentrated in the extreme ultraviolet (EUV) and X-ray bands [2]. The X-ray radiation reflects the progression of change in the high-temperature plasma of the corona [3]. The effects of the 19.5-nm EUV spectrum on the observation of certain solar activities or phenomena that are accompanied by outbreaks of activity in the sun are very prominent and can make up for a lack of X-ray observation [4]. Therefore, instruments for observation of the sun are generally focused on operation in the X-ray and EUV bands.

The XEUVI is an important remote sensing instrument on the Fengyun-3 satellite. The mission and function of the XEUVI will be to use the X-ray and EUV bands of solar radiation to achieve long-term, continuous, and high time resolution of full-day and low-day imaging observations, to obtain high-resolution images of the sun and to provide a reference for more accurate spatial weather prediction. With high photon energy and the refractive index of all materials being close to one, grazing incidence focusing can only

* Corresponding author at: Changchun Institute of Optics, Fine Mechanics and Physics, Chinese Academy of Sciences, Changchun, Jilin, 130033, China.
E-mail addresses: 1228666705@qq.com (S. Li), chenliheng3@163.com (L. Chen), yangyuting171@mails.ucas.ac.cn (Y. Yang).
[1] Professor, Thermal Control Group.
[2] Master Degree Candidate, Thermal Control Group.

https://doi.org/10.1016/j.ijleo.2019.164017
Received 29 October 2019; Accepted 6 December 2019

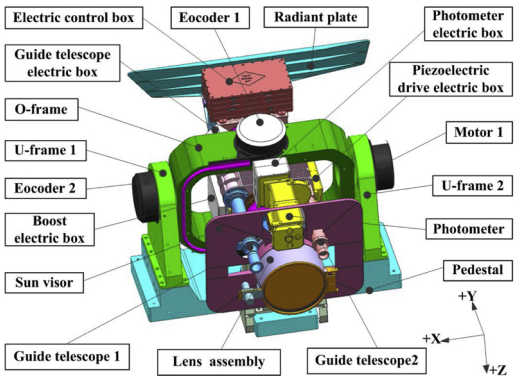

Fig. 1. Structure of XEUVI.

be adopted for imaging in the X-ray band. However, positive incidence focusing can be used for imaging in the EUV band. The same set of image sensors is used for both bands. An integrated imager design for both the positive incidence and grazing incidence was first proposed internationally and was successfully designed in China.

The thermal control of the XEUVI will be implemented by a sun visor mounted on the front end of the lens tube to isolate the direct solar heat flux. In addition, a radiant plate will be installed at the rear of the lens tube to ensure that CCD operates at a low temperature. During the thermal analysis, the external heat fluxes of different attitudes were considered comprehensively [5]. In the thermal design process, the difficulties of thermal design were first analyzed. Then, according to the difficulties of thermal design, a corresponding thermal design scheme was proposed. Finally, the detailed thermal design of each part was carried out. To meet the requirements of CCD in low temperature operation, a heat dissipation device is designed for CCD, which is not only satisfies the requirement of large temperature difference of 80 °C between CCD and surrounding components, but also meets the requirements of CCD to achieve small motion in three directions of X, Y and Z. The entire thermal design of the XEUVI is adopted with a combination of active and passive thermal controls [6], and the thermal design was verified by a thermal balance test [7], completing the thermal control design task for the XEUVI system.

2. Overview of the XEUVI

Structure of the XEUVI

The structure of the XEUVI, shown in Fig. 1, includes an imaging subsystem, pointing mechanism subsystem, and electronic control box subsystem. The imaging subsystem mainly includes a lens assembly, guide telescope assembly, photometer assembly, and CCD assembly. The pointing mechanism subsystem mainly includes a pedestal, two U-frames, an O-frame, two pointing motors, and two encoders. The electronic control box subsystem mainly includes a control electric box, piezoelectric drive electric box, boost electric box, guide mirror electric box, photometer electric box, and signal processing box. Among them, the role of the guide telescope is to image the sun and correct the error caused by the long-term tracking of the sun by the optical axis. The function of the photometer is to measure the radiation flow generated by the X-ray and EUV bands. The pedestal, U-frame, O-frame, and lens tube are made of a carbon fiber composite, which not only effectively reduces thermal deformation but also reduces weight. The guide telescope, photometer, electric boxes, and motors are made of aluminum alloy to reduce their temperature gradient.

Working mode

The XEUVI will work in a sun-synchronous orbit with a track height of 836 km and an orbit inclination of 98.76°, and the local time of the satellite through the ascending node is 5:40 am.The XEUVI's forward flight direction is defined as the + X direction, whereas the direction toward the ground is defined as the + Z direction, and the + Y direction is determined by the right-hand rule.

For the XEUVI detection head scanning field of view, the angle between the field of view axis and the -Y axis is not more than 33°. Because the angle between the field of view axis and the XOY surface of the satellite is from -9° (+Z) to +33° (-Z), the field of view is not obstructed, as shown in Fig. 2.

When the XEUVI will operate on orbit, the field of view of the XEUVI is guaranteed by its position on the satellite platform. It is necessary to ensure that each track lasts for at least 50 min. In 1 year, the changes of observing the sun's time for XEUVI and β-angle with date are shown in Fig. 3. The maximum beta angle (β_{max}) and the minimum beta angle (β_{min}) are given in Table 1.

Internal heat sources

The internal heat sources of the XEUVI include the CCD, two pointing motors, piezoelectric drive electric box, boost electric box, guide telescope electric box, photometer electric box, and signal processing box. The power of these internal heat sources is shown in Table 2.

3. Thermal design

Thermal Design Difficulties

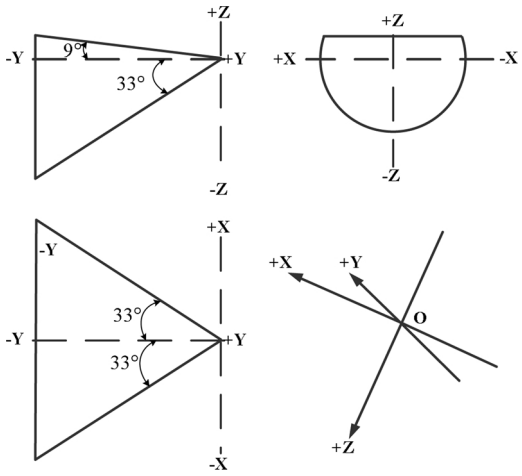

Fig. 2. Schematic diagram of XEUVI detection head field of view.

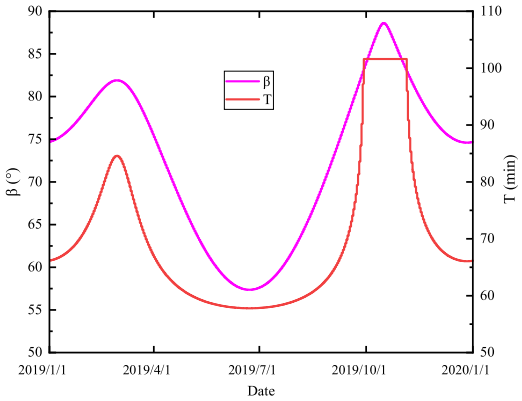

Fig. 3. XEUVI observation of the sun's time and β-angle change with date in 1 year.

Table 1
Times and angles of β_{max} and β_{min}.

Name	Time	Angle
β_{min}	2019/06/22 22:50	57.4°
β_{max}	2019/10/16 10:04	88.6°

Table 2
Power of internal heat source (units : W).

Source	CCD	Pointing motors	Control electric box	Piezoelectric drive electric box	Boost electric box	Guide telescope electric box	Photometer electric box	Signal processing box
Power	0.446	3 × 2	25	8.6	6.9	2.5	4.9	3.5

The thermal design difficulties of the XEUVI mainly include the following aspects: (1) When the XEUVI operates on orbit, its attitude is constantly changing due to the requirement that its optical axis must always point to the center of the sun. Therefore, the direct solar heat flux of light entrance is very large. (2) The temperature requirement of the CCD is about -60 °C, and its surrounding assemblies will be around 20 °C, which will create a large temperature difference between them. Therefore, it is difficult to maintain a constant low temperature for the CCD. (3) The electric box and motor will consume a large amount of power and operate for long periods; simultaneously, they will be affected by complicated external heat fluxes, which will make heat dissipation difficult.

Lens assembly

Because the optical axis of the XEUVI always points to the center of the sun when it operates on orbit, the front end of the lens has a large solar direct heat flux. To shield the lens from this energy, a sun visor is installed at the front end of the lens tube, while a filter

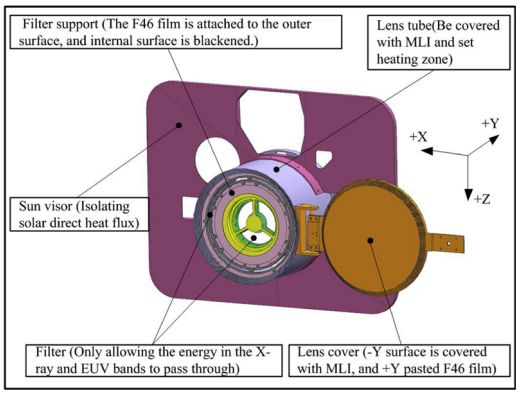

Fig. 4. Schematic diagram of the thermal design of the lens assembly.

assembly is installed at the front end of the lens. The sun visor can effectively isolate the solar direct heat flux, so that the assemblies behind the visor have a lower-temperature thermal environment. The filter only allows energy in the X-ray and EUV bands to pass through, and the energy in the remaining bands is blocked, minimizing the effect of energy on the internal optical elements. A polyimide film (F46) is attached to the filter support surface, and the inside of the filter is blackened, which reduces the temperature of the filter assembly. To ensure the stability of the temperature of the optical elements inside the lens, the surface of the lens tube is covered with multi-layer insulation (MLI) to isolate it from the space environment, while a heating zone is set on the lens tube to control the temperature of the lens tube to about 20 °C. In addition, to reduce the influence of the lens cover on the lens tube, an aluminum film is attached to the -Y surface of the lens cover, and the + Y surface covers the 20-layer MLI. A schematic diagram of the thermal design of the entire lens assembly is shown in Fig. 4.

Pointing mechanism

The boundary temperature of the satellite platform interface will vary widely over the range from -20 °C to 45 °C. To reduce the influence of the satellite platform on the XEUVI, the pedestal and the satellite platform are thermally insulated by a polyimide insulation pad 10 mm thick, and a heating zone is set on the pedestal to control the temperature to about 10 °C. The power consumption of motors 1 and 2 are both 3 W, and the temperature will rise faster when they work for a long time. To control the temperature of the motor within the allowable temperature range, a heat dissipation surface is opened in the motor 1 housing in the + Y direction. The bottom of motor 2 is the pedestal, and its position is not conducive to heat dissipation. Therefore, in addition to the heat dissipation surface of the + Y direction of the motor 2 housing, an ammonia channel heat pipe made of aluminum is used, as shown in Fig. 5. In this way, part of the heat of motor 2 is dissipated through the heat dissipation surface, and the other part of the heat is transmitted to the encoder for dissipation through the heat pipe. To prevent the temperature of the motor, U-frame, and O-frame from being too low, heating zones are set on the surfaces to increase the temperature as needed. The outside of the pointing mechanism (except for the heat dissipation surface and the mounting surface) is covered with MLI to reduce the impact of the space environment.

Guide telescope and photometer

As important parts of the XEUVI, the temperature stability requirements of the guide telescope and photometer are very high. The guide telescope and photometer are mounted on the primary optical tube with insulation, while their outer surfaces are covered with MLI.

The front end of the guide telescope is equipped with a sunshade blackened inside, which eliminates stray light and improves the

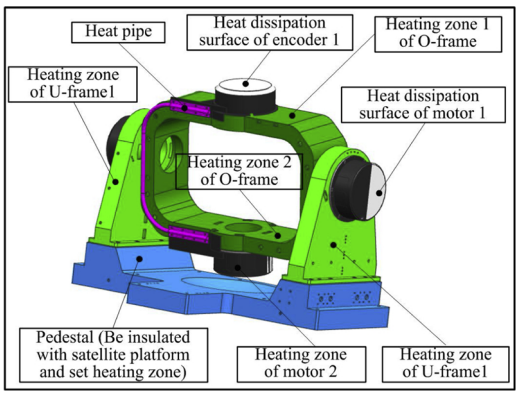

Fig. 5. Schematic diagram of thermal design of the pointing mechanism.

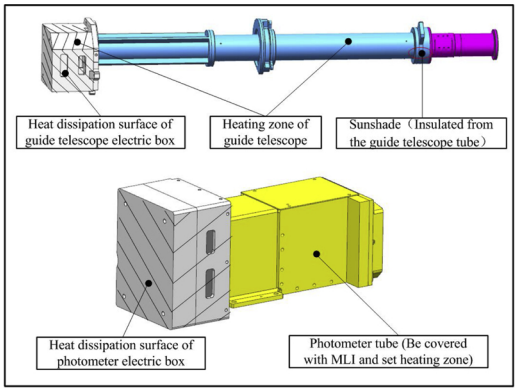

Fig. 6. Schematic diagram of guide telescope and photometer thermal design.

imaging quality of the guide telescope. The guide telescope keeps track of the sun as the instrument orbits, and the front end sunshade will absorb more energy. To reduce the influence of the sunshade on the tube of the guide telescope, the sunshade and tube are insulated by the heat insulation pad. The front end of the photometer is equipped with a filter wheel, and it is rotated to select light of different wavelengths.

Both the guide telescope and the photometer have imaging electric boxes (power consumption of 2.5 W and 4.9 W, respectively), which are both insulated from the front telescope tube. To avoid the temperature of imaging box of and the photometer becoming too high, heat dissipation surfaces are set on the surfaces of the imaging electric box. The heat dissipation surface of the imaging electric box of the guide telescope is the whole surface and the heat dissipation surface of the imaging electric box of the photometer opens to the + X and + Y directions. In addition, to meet the requirements of the temperature stability of the guide telescope and the photometer, heating zones are provided on their surfaces, as shown in Fig. 6.

Electrical box

There are a total of six electric boxes. Only the control electric box (25 W), boost electric box (6.9 W), and piezoelectric drive electric box (8.6 W) are discussed here. The control electric box is installed in the + Z plane of the box with insulation, and both the boost electrical box and piezoelectric drive box are thermally insulated from the primary optical tube support. Because the electric box will operate for long periods and generate a large amount of heat, it is necessary to take certain measures to dissipate heat. Although the control electric box will consume a large amount of power, due to its large size, its temperature can be controlled within the allowable range simply by opening a heat dissipation surface on its surface. The piezoelectric drive electric box and boost electric box, because of their relatively small size, cannot meet their temperature requirements even if all the surfaces (except the mounting surfaces) are used as heat dissipation surface. Therefore, the heat dissipation fins shown in Fig. 7 are attached to the piezoelectric drive electric box and the boost electric box for heat dissipation.

CCD assembly

3.1. Structure of the CCD assembly

The CCD and its surrounding related structure are shown in Fig. 8. The CCD assembly mainly includes the CCD, focal plane substrate, thermal aluminum block, thermal straps, radiant plate, signal processing box ect. There is an optical tube at the front end of the box and a control box at the upper end.

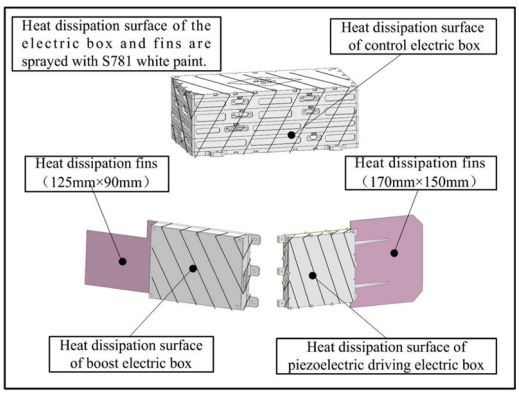

Fig. 7. Schematic diagram of the thermal design of the electrical box.

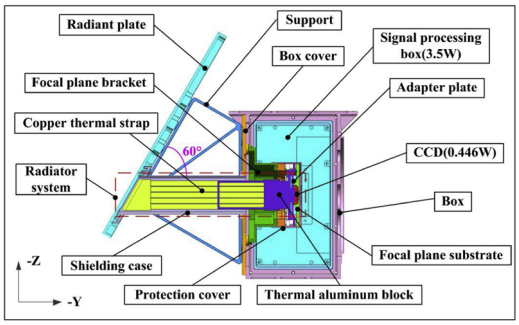

Fig. 8. Structure of CCD assembly.

3.2. Passive cooling scheme

As a key element of the entire optical system, the CCD requires a temperature range of -70 °C – -50 °C. To meet the requirements of CCD in low temperature operation, a heat dissipation device is designed for CCD, including CCD, thermal aluminum block, thermal straps, radiant plate. The device not only satisfies the requirement of large temperature difference of 80 °C between CCD and surrounding components, but also meets the requirements of CCD to achieve small motion in three directions of X, Y and Z.

In the thermal design process, on the one hand, the heat transferred to the CCD and the influence on the heat dissipation path of the CCD are reduced as much as possible, through thermal insulation measures. On the other hand, the heat generated by the CCD is dissipated in time and the CCD is guaranteed to meet the operation temperature, through thermal conduction measures.

The measures for thermal insulation are as follows: 1) the CCD and thermal aluminum block are insulated from the focal plane substrate; 2) the focal plane substrate and bracket are thermally insulated by a polyimide insulation pad; 3) the bracket and radiant plate are insulated from the cover of the box; 4) The thermal aluminum block are gold-plated and covered with three units of MLI; 5) The thermal straps and inner surface of the box are also covered with three units of MLI.

Interfaces between the CCD and thermal aluminum block, thermal aluminum block and thermal straps, and thermal straps and radiant plate are both thermally conductive and filled with thermal conduction filler.

Fig. 9 is a schematic diagram of the thermal design heat transfer path of the CCD assembly (radiation heat exchange path between components is not shown), which depicts the path of heat generated by the internal heat source in the CCD assembly to space. Among them, R1 – R16 are the thermal resistances between the assemblies, the solid line indicates conduction, and the broken line indicates radiation. As can be seen from Fig. 9, part of the heat in the CCD assembly is radiated to cold space by the radiant plate, and the other portion is radiated to space through the heat dissipation surface of the side plate of the box.

4. Thermal balance test

Test scheme

In the thermal balance test for the XEUVI, the space environment was simulated with a space environment simulator and the absorbed external heat fluxes were simulated by heaters [8][9] [10]. The external heat fluxes absorbed by the MLI surfaces were simulated by heaters attached to the outer surfaces. The external heat fluxes absorbed by the light entrances (including the entrances of the primary optical tube, guide telescope, and photometer) were also simulated by attaching a heater to their surfaces. In addition, the satellite platform was simulated by an aluminum plate10 mm thick, whose temperature was controlled by attaching heaters to its surface and simultaneously insulating it from the pedestal. Fig. 10 is a physical layout of the XEUVI's thermal balance test, including

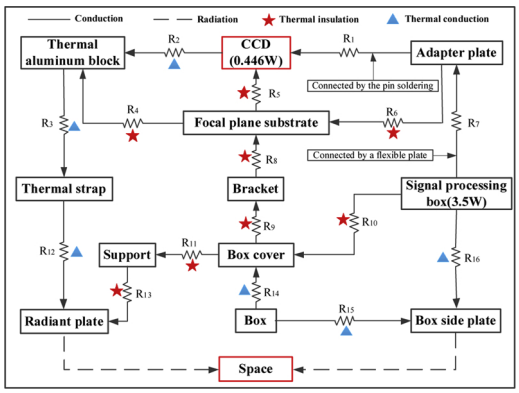

Fig. 9. Schematic diagram of the thermal design heat transfer path of the CCD assembly.

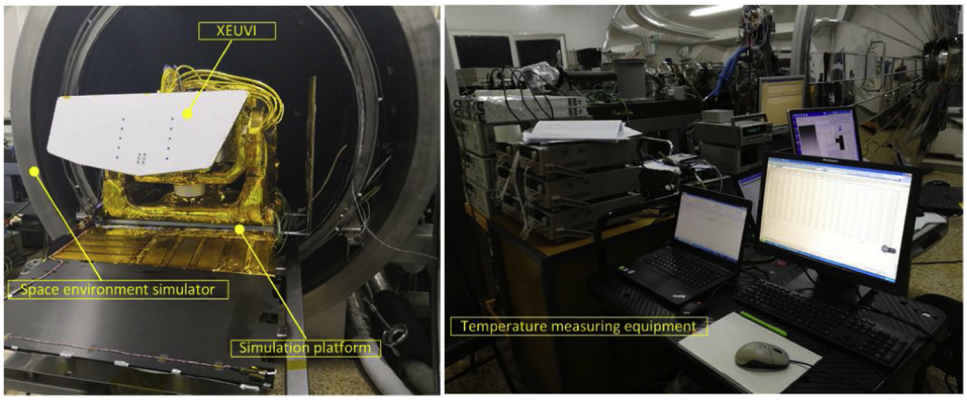

Fig. 10. Physical layout of the thermal balance test.

Table 3
Description of test equipment.

Number	Equipment name	Main function
1	Space environment simulator	Simulated vacuum environment and cold black background
2	Main control box	Measuring and temperature control of test pieces
3	Comprehensive simulation equipment	Testing and detecting
4	Keithley temperature measuring equipment	Measuring temperature and collecting data by thermocouple
5	Power supply equipment	Providing heating power

Table 4
Thermal balance test conditions.

No.	Condition name	Main setting conditions
1	Low-temperature 1 (LT1)	β=88.6°, S = 1414 W/m^2, F46 ($\alpha s/\varepsilon$ = 0.15/0.69), S781 ($\alpha s/\varepsilon$ = 0.17/0.86), T= -20 °C.
2	Low-temperature 2 (LT2)	β=57.4°, S = 1322 W/m^2, F46 ($\alpha s/\varepsilon$ = 0.15/0.69), S781 ($\alpha s/\varepsilon$ = 0.17/0.86), T= -20 °C.
3	Low-temperature 3 (LT3)	T= -30 °C. The external heat flux is 70% of the LT 1, and the rest settings are the same as the LT 1.
4	High-temperature 1 (HT1)	β=88.6°, S = 1414 W/m^2, F46 ($\alpha s/\varepsilon$ = 0.36/0.69), S781 ($\alpha s/\varepsilon$ = 0.40/0.86), T=45 °C.
5	High-temperature 2 (HT2)	β=57.4°, S = 1322 W/m^2, F46 ($\alpha s/\varepsilon$ = 0.36/0.69), S781 ($\alpha s/\varepsilon$ = 0.40/0.86), T=45 °C.
6	High-temperature 3 (HT3)	T=55 °C. The external heat flux is 130% of the HT 2, and the rest settings are the same as the HT 2.

the XEUVI, space environment simulator, simulation platform, and test equipment. The specific test devices and their functions are described in Table 3.

Thermal balance test conditions

Six extreme conditions were simulated by varying the external heat fluxes, working mode, distribution of internal heat sources, and thermal properties of the thermal control layer. The specific settings are listed in Table 4, main including the β-angle (β), solar constant (S), performance parameter of F46 membrane (F46), performance parameter of S781 white paint (S781), temperature of simulated platform (T). The internal heat source and the active thermal control always work.

Test Results and Analysis

According to the designed conditions, the thermal balance test was completed in the order from low temperature to high temperature. The degree of vacuum during the thermal balance test was 5×10^{-5} Pa, and the heat sink temperature was 100 K. The test results are shown in Fig. 11 as temperature curves of the key components of the XEUVI under different conditions.

At the same time, according to the test results, the temperature data the key components under various condition were also compiled, including CCD, optical system (including lens tube, guide telescope, and photometer), frame (including U-frame and O-frame), motor (including motor 1 and motor 2) and the electrical box (including boost electric box and piezoelectric drive electric box), as shown in Table 5.

When the β angle is 57.4°, the orbit has a shadow area of 16.7 min, the external heat flux changes greatly, and the lens rotation

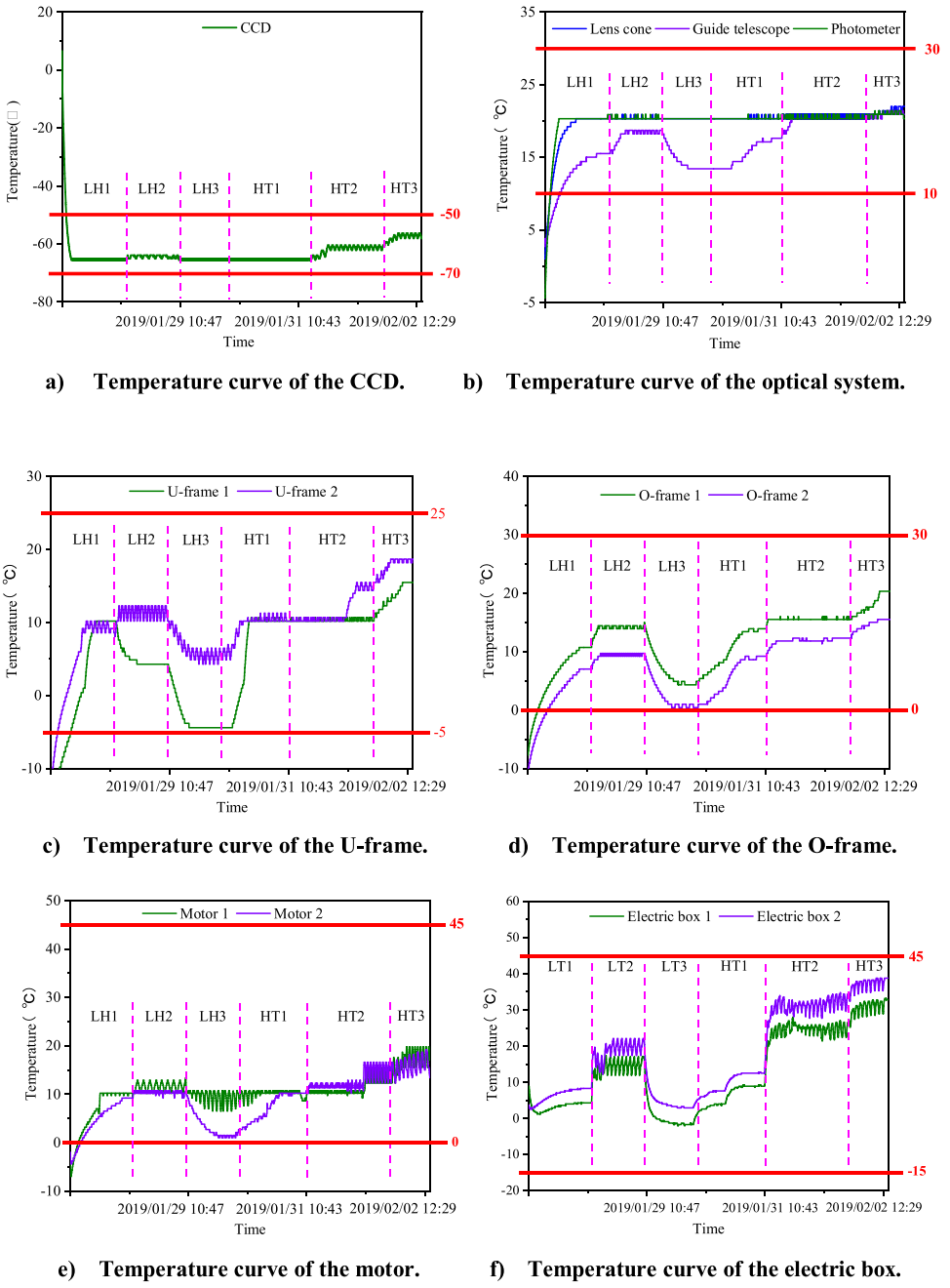

a) Temperature curve of the CCD.

b) Temperature curve of the optical system.

c) Temperature curve of the U-frame.

d) Temperature curve of the O-frame.

e) Temperature curve of the motor.

f) Temperature curve of the electric box.

Fig. 11. Temperature curve of the key components.

angle is large. A full sunshine orbit is achieved when the β angle is 88.6°. In this case, the external heat flux is relatively stable and the lens rotation angle is small. Since the motor, electric box and CCD's radiant plate have heat dissipation surfaces, their temperatures are greatly affected by the external heat flux. when the β angle is 57.4°, the external heat flux changes greatly due to the large rotation angle. Thus, the temperatures of the motor, electric box and CCD fluctuate greatly than at the β angle of 88.6°. The remaining components are coated with MLI and are less affected by external heat flux, so their temperature fluctuations are small.

At the same time, it can be seen from Table 8 that the CCD temperature ranges from -65.6 ℃ to -56.3 ℃, the optical system temperature ranges from 12.9 ℃ to 22.0 ℃, the frame temperature ranges from -4.6 ℃–20.3 ℃, the motor temperature ranges from 1.0 ℃ to 19.8 ℃, and the electrical box temperature ranges from -2.0 ℃–38.8 ℃, which all meet the thermal control indices.

During the test, the turntable pointing is related to the β angle. When the β angle is 88.6°, the pointing mechanism rotates at a small angle, including LT1, LT3 and HT1. While the β angle is 57.4°, the pointing mechanism rotates at a large angle, including LT2, HT2 and HT3. According to the test results, the rotation angle (pitch angle/azimuth angle) and the current of the turntable motor

Table 5
Temperature of key components (units : ℃).

Name	β = 88.6°			β = 57.4°			Indices
	LT 1	LT 3	HT1	LT2	HT2	HT3	
CCD	−65.6 – -65.1	−65.6 – -65.1	−65.6 – -65.1	−65.1 – -63.9	−62.2 – -60.4	−58.1 – -56.3	−70 – -50
Lens cone	19.8 – 20.3	19.8 – 20.3	20.3 – 20.9	20.3 – 20.9	20.3 – 20.9	21.4 – 22.0	10 – 30
Guide telescope	15.0 – 15.5	12.9 – 13.4	17.1 – 17.6	18.2 – 18.7	20.3 – 20.9	20.9 – 21.4	10 – 30
Photometer	19.8 – 20.3	20.3 – 20.9	20.3 – 20.9	20.3 – 20.9	20.3 – 20.9	20.3 – 21.4	10 – 30
U-frame 1	9.7 – 10.2	−4.6 – -4.1	10.2 – 10.7	4.3 – 4.8	10.2 – 11.3	15.0 – 15.5	−5 – 25
U-frame 2	8.6 – 10.2	4.3 – 6.5	10.2 – 11.3	10.2 – 12.3	14.4 – 15.5	18.2 – 18.7	−5 – 25
O-frame 1	10.2 – 10.7	4.3 – 4.9	13.4 – 13.9	13.9 – 14.4	15.5 – 16.0	19.8 – 20.3	0 – 30
O-frame 2	6.5 – 7.0	0.4 – 1.0	8.6 – 9.2	9.2 – 9.7	12.3 – 12.9	15.0 – 15.5	0 – 30
Motor 1	9.7 – 10.2	6.5 – 10.7	8.6 – 10.7	10.2 – 12.9	12.3 – 15.5	15.5 – 19.8	0 – 45
Motor 2	8.7 – 9.2	1.0 – 1.5	9.7 – 10.2	9.7 – 10.2	12.3 – 16.6	13.4 – 19.2	0 – 45
Piezoelectric drive electric box	4.0 – 4.3	−2.0 – -0.6	8.9 – 9.3	11.9 – 17.1	22.4 – 27.0	28.9 – 33.2	−15 – 45
Boost electric box	8.0 – 8.3	2.9 – 3.6	12.5 – 12.8	17.4 – 22.1	29.6 – 34.8	35.3 – 38.8	−15 – 45

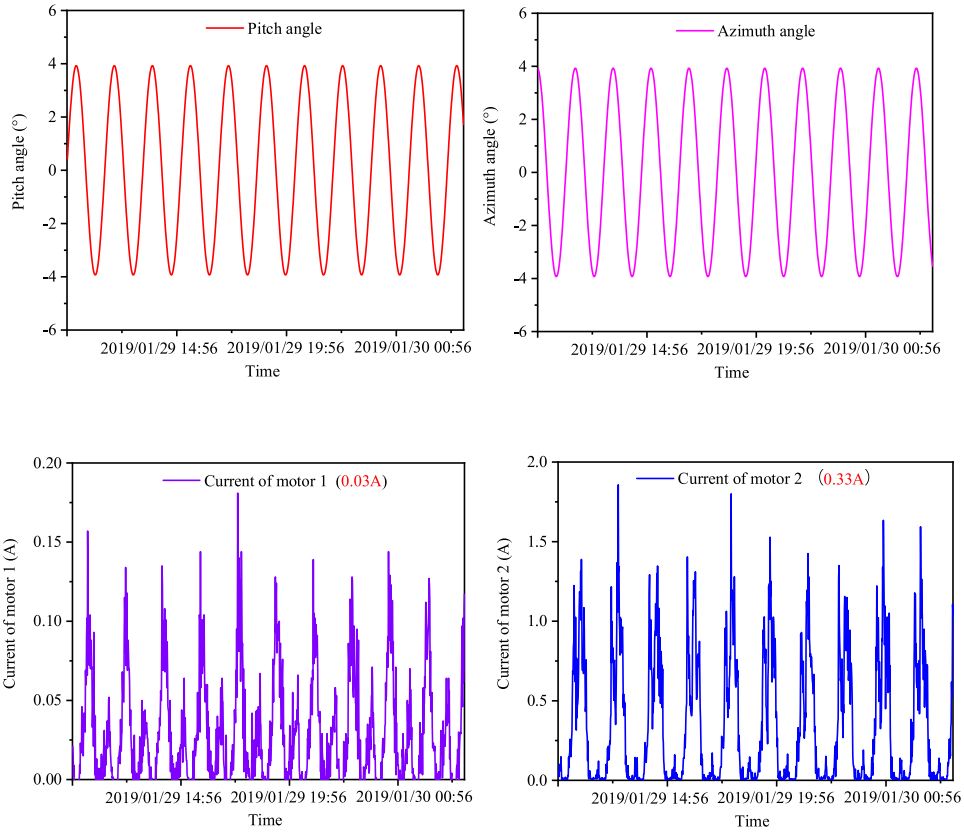

Fig. 12. Rotation angle and current at the angle of 88.6°.

under different β angles are counted, as shown in Figs. 12–13. It can be seen from the figures that when the β angle is 88.6°, the rotation range of the pitch angle and the azimuth angle are both form -4° to +4°. When the β angle is 57.4°, the rotation range of the pitch angle is from -31° to +31°, and the azimuth angle from -8.3° to +31°. The current of the motor 1 is smaller than that of the motor 2, and the current of the motor at the β angle of 88.6° is smaller than that at the β angle of 57.4°. The average currents of motor 1 and motor 2 at the angle of 88.6° are 0.03A and 0.33A, respectively, and at the angle of 88.6°, 0.15A and 1.0A.

5. Conclusion

The detailed thermal design scheme of the XEUVI was proposed according to the space environment, the XEUVI structural characteristics and working modes. In general, its thermal design mainly uses passive thermal control measures for thermal

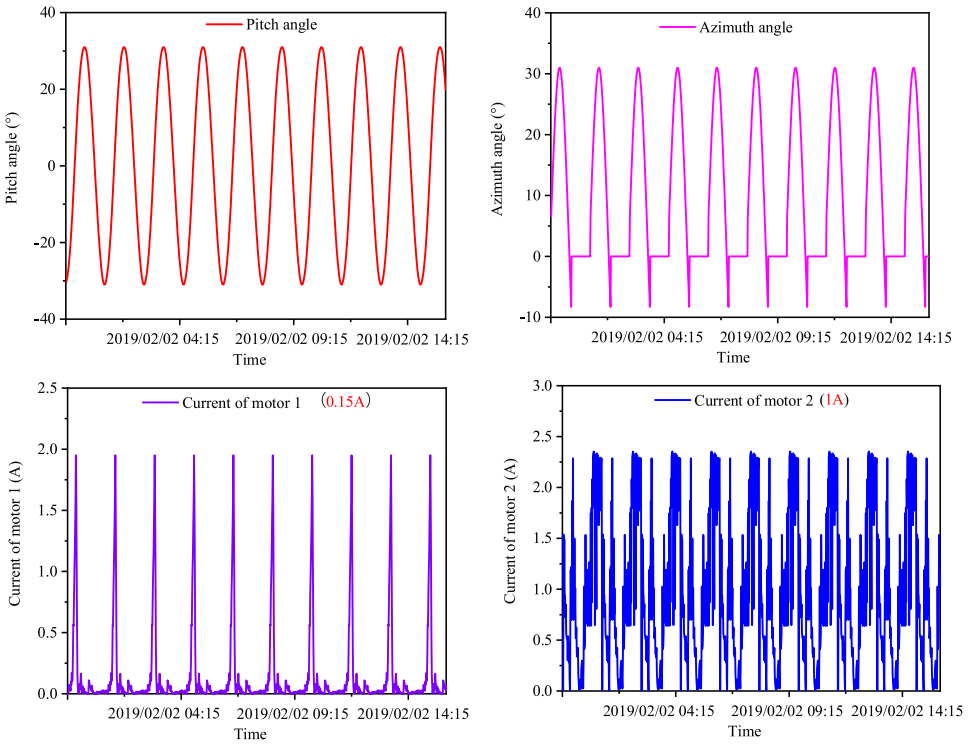

Fig. 13. Rotation angle and current at the angle of 57.4°.

insulation, thermal conduction, and thermal dissipation. At the same time, active thermal control measures are used for temperature difference compensation.

To verify the correctness of the thermal design, the XEUVI was subjected to a thermal balance test according to the six planned conditions. The results of the thermal balance test indicate that the CCD temperature ranges from -65.6 ˚C to -56.3 ˚C, the optical system temperature ranges from 12.9 ˚C to 22.0 ˚C, the frame temperature ranges from -4.6 ˚C–20.3 ˚C, the motor temperature ranges from 1.0 ˚C to 19.8 ˚C, and the electrical box temperature ranges from −2 ˚C to 38.8 ˚C. All these values meet the requirements of the thermal control indices, verifying the correctness of the thermal design.

Declaration of competing Interest

No conflict of interest exits in the submission of this manuscript, and manuscript is approved by all authors for publication.

Acknowledgments

The work is supported by National Key R&D Program of China under Grant No. 2018YFB0504800. We would like to thank all the members for contributing to the development of the Solar X-Ray and Extreme Ultraviolet Imager.

References

[1] J.L. Peng, G.W. Zhu, F. Wei, B.Q. Li, Solar extreme ultraviolet multichannel imager, Chinese Journal, Space Science 29 (No. 4) (2009) 417–421.
[2] B.Q. Li, G.W. Zhu, S.J. Wang, H.A. Lin, J.L. Peng, J. Liu, The solar X-EUV imaging telescope, Chinese Journal. Geophys. Vol. 48 (No. 2) (2005) 235–242.
[3] G. Huang, H. Zhang, J. Yang, Thermal Design and Analysis of a Hard X-Ray Modulation Telescope, J. Thermophys. Heat Transf. 22 (No. 3) (2015) 528–530.
[4] J.F. Seely, D. Windt, S. Donguy, C. Brown, G. Hlland, W. Hunter, Performance of multilayer-coated gratings for the extreme-ultraviolet imaging spectrometer (EIS) for the solar-B mission, Proceedings of Society of Photo-Optical Instrumentation Engineers 5168 (2004).
[5] S.J. Li, L.H. Chen, Y.H. Wu, Calculation of external heat fluxes on space camera with two-dimensional changing attitudes in sun-synchronous orbit, Infrared Laser Eng. 47 (No. 9) (2018) 286–295.
[6] C. Sun, Z.Y. Wang, X. Chen, X.L. Xia, A passive thermal control method by radiative shield with multi-parameter adjustment capacity, Appl. Therm. Eng. 94 (2016) 600–606.
[7] Y. Gao, B. Zhang, L. Chen, et al., Thermal design and analysis of the high resolution MWIR/LWIR aerial camera, Opt. – Int. J. Light Electron. Opt. (2019) 37–46.
[8] T. Beck, A. Bieler, N. Thomas, Numerical thermal mathematical model correlation to thermal balance test using adaptive particle swarm optimization (APSO), Appl. Therm. Eng. 38 (2012) 168–174.
[9] E. Emanuel, M. Diaz, J.C. Zagal, Evolutionary design of a satellite thermal control system: Real experiments for a cubesat mission, Appl. Therm. Eng. 105 (2016) 490–500.
[10] D. Park, K. Miyata, H. Nagano, Thermal design and validation of radiation detector for the ChubuSat-2micro-satellite with high-thermal-conductive graphite sheets, Acta Astronaut. 136 (2017) 387–394.